

Structured and Gradient Polymer Brushes from Biphenylthiol Self-Assembled Monolayers by Self-Initiated Photografting and Photopolymerization (SIPGP)

Marin Steenackers,[†] Alexander Küller,[‡] Svetlana Stoycheva,[‡] Michael Grunze,^{*,‡} and Rainer Jordan^{*,†,§}

Wacker-Lehrstuhl für Makromolekulare Chemie, Technische Universität München, Lichtenbergstraße 4, 85747 Garching, Germany, and Lehrstuhl für Angewandte Physikalische Chemie, Universität Heidelberg, Im Neuenheimer Feld 253, 69120 Heidelberg, Germany

Received October 14, 2008. Revised Manuscript Received December 4, 2008

The self-initiated photografting and photopolymerization (SIPGP) of styrene, methyl methacrylate, and *tert*-butyl methacrylate on structured self-assembled monolayers (SAMs) of electron beam cross-linked ω -functionalized biphenylthiols SAMs on gold was investigated. Polymer brushes with defined thickness can be prepared on cross-linked benzyl-, phenyl-, hydroxyl-, and amino-functionalized SAMs, whereas non-cross-linked SAM regions desorb from the surface during the SIPGP process. By the preparation of brush gradients on different functionalized SAMs, it was demonstrated that the resulting polymer brush layer thickness is determined by the locally applied electron beam dosage. Defined micro-nanostructured polymer brush patterns can be prepared down to a size of 50 nm. Finally, it was shown that polymer brushes obtained by the SIPGP process have a branched architecture.

Introduction

Surface-initiated polymerization (SIP) on organic and inorganic substrates has been widely used for the preparation of stable and functional polymer coatings.¹ SIP has been used to synthesize hyperbranched² as well as linear polymers by various routes including free³ and controlled⁴ radical, living anionic,⁵ and living cationic⁶ polymerization.

Recently, the fabrication of patterned polymer brushes for micro- and nanotechnology applications gained much interest.⁷ Such surfaces can be fabricated on structured self-assembled monolayers (SAMs) prepared, for example, by microcontact

printing,⁸ two-dimensional gradients,⁹ scanning probe microscopy techniques,¹⁰ or chemical lithography with electron irradiation^{11–16} and subsequent SIP using the SAM structure as a 2D initiator template. The surface selectivity of the SIP reaction is ensured by the specific end-functionalization of the structured SAM with a suitable initiator group.

Rånby and co-workers developed the bulk surface photografting polymerization process.¹⁷ This single-step procedure allows the formation of micrometer thick polymer brushes directly from native cross-linked polymer substrates such as polyethylene, poly(ethylene terephthalate), nylon, polypropylene, and polyvinylchloride without preimmobilization of initiators onto the substrate. The polymer brushes were formed by a simple and fast procedure: the substrate was placed in bulk monomer with benzophenone (BP) as a photosensitizer and irradiated with UV light of a spectral distribution between 300 and 400 nm.¹⁸ Later, the same group reported that the concentration of the additive, BP, had only a slight effect on the grafting efficiency of, for example, styrene on polyethylene substrates.¹⁹ The same grafting

* To whom correspondence should be addressed. Fax: +49-89 289 13562 (R.J.); +49-6221 54 6199 (M.G.). E-mail: Rainer.Jordan@ch.tum.de (R.J.); Michael.Grunze@urz.uni-heidelberg.de (M.G.).

[†] Technische Universität München.

[‡] Universität Heidelberg.

[§] Current address: Professur für Makromolekulare Chemie, Department Chemie, Technische Universität Dresden, 01062 Dresden, Germany.

(1) (a) *Surface-Initiated Polymerization I & II*; Jordan, R., Ed.; Advances in Polymer Science Series; Springer: Berlin, 2006; Vols. 197 & 198. (b) *Polymer Brushes*; Advincula, R. C., Brittain, W. J., Caster, K. C., Rühle, J., Eds.; Wiley-VCH: Weinheim, 2004.

(2) (a) Bergbreiter, D. E.; Kippenberger, A. M. *Adv. Polym. Sci.* **2006**, *198*, 1–49. (b) Matsuda, T. *Adv. Polym. Sci.* **2006**, *197*, 67–106. (c) Mori, H.; Müller, A. H. E. *Polymer Brushes* **2004**, 167.

(3) (a) Fery, N.; Hoene, R.; Hamann, K. *Angew. Chem., Int. Ed.* **1972**, *11*, 337. (b) Laible, R.; Hamann, K. *Adv. Colloid Interface Sci.* **1980**, *13*, 65. (c) Prucker, O.; Rühle, J. *Macromolecules* **1998**, *31*, 592. (d) Prucker, O.; Rühle, J. *Langmuir* **1998**, *14*, 6893–6898.

(4) (a) Zhao, B.; Brittain, W. J. *J. Am. Chem. Soc.* **1999**, *121*, 3557. (b) Matyjaszewski, K.; Miller, P. J.; Shukla, N.; Immaraporn, B.; Gelman, A.; Luokala, B. B.; Siclvan, T. M.; Kickelbick, G.; Vallant, T.; Hoffmann, H.; Pakula, T. *Macromolecules* **1999**, *32*, 8716. (c) Husseman, M.; Malmstroem, E. E.; McNamara, M.; Mate, M.; Mecerreyes, D.; Benoit, D. G.; Hedrick, J. L.; Mansky, P.; Huang, E.; Russell, T. P.; Hawker, C. J. *Macromolecules* **1999**, *32*, 1424–1431.

(5) (a) Jordan, R.; Ulman, A.; Kang, J. F.; Rafailovich, M.; Sokolov, J. *J. Am. Chem. Soc.* **1999**, *121*, 1016. (b) Advincula, R.; Zhou, Q.; Park, M.; Wang, S.; Mays, J.; Sakellariou, G.; Pispas, S.; Hadjichristidis, N. *Langmuir* **2002**, *18*, 8672–8684. (c) Advincula, R. *Adv. Polym. Sci.* **2006**, *197*, 107–136.

(6) (a) Jordan, R.; Ulman, A. *J. Am. Chem. Soc.* **1998**, *120*, 243. (b) Jordan, R.; West, N.; Ulman, A.; Chou, Y. M.; Nuyken, O. *Macromolecules* **2001**, *34*, 1606.

(7) Nie, Z.; Kumacheva, E. *Nat. Mater.* **2008**, *7*, 277–290.

(8) Husemann, M.; Mecerreyes, D.; Hawker, C. J.; Hedrick, J. L.; Shah, R.; Abbott, N. L. *Angew. Chem., Int. Ed.* **1999**, *38*, 647–649.

(9) Bhat, R. R.; Tomlinson, M. R.; Wu, T.; Genzer, J. *Adv. Polym. Sci.* **2006**, *198*, 51–124.

(10) (a) Liu, X.; Guo, S.; Mirkin, C. A. *Angew. Chem., Int. Ed.* **2003**, *42*, 4785–4789. (b) Kaholek, M.; Lee, W.; LaMattina, B.; Caster, K. C.; Zauscher, S. *Nano Lett.* **2004**, *4*, 373–376.

(11) Schmelmer, U.; Jordan, R.; Geyer, W.; Eck, W.; Götzhäuser, A.; Grunze, M.; Ulman, A. *Angew. Chem., Int. Ed.* **2003**, *42*, 559.

(12) Schmelmer, U.; Paul, A.; Küller, A.; Steenackers, M.; Ulman, A.; Grunze, M.; Götzhäuser, A.; Jordan, R. *Small* **2007**, *3*, 459–465.

(13) Steenackers, M.; Küller, A.; Ballav, N.; Zharnikov, M.; Grunze, M.; Jordan, R. *Small* **2007**, *3*, 1764.

(14) (a) He, Q.; Küller, A.; Grunze, M.; Li, J. *Langmuir* **2007**, *23*, 3981–3987. (b) He, Q.; Küller, A.; Schilp, S.; Leisten, F.; Kolb, H. A.; Grunze, M.; Li, J. *Small* **2007**, *3*, 1860–1865.

(15) (a) Kaholek, M.; Lee, W.; Feng, J.; LaMattina, B.; Dyer, D. J.; Zauscher, S. *Chem. Mater.* **2006**, *18*, 3660–3664. (b) Ahn, S. J.; Kaholek, M.; Lee, W.; LaMattina, B.; LaBean, T. H.; Zauscher, S. *Adv. Mater.* **2004**, *16*, 2141–2145.

(16) Ballav, N.; Schilp, S.; Zharnikov, M. *Angew. Chem., Int. Ed.* **2008**, *47*, 1421.

(17) Yang, W.; Rånby, B. *J. Appl. Polym. Sci.* **1996**, *62*, 533.

(18) Yang, W. T.; Rånby, B. *Polym. Bull.* **1996**, *37*, 89.

(19) Deng, J.-P.; Yang, W.-T.; Rånby, B. *Macromol. Rapid Commun.* **2001**, *22*, 535.

efficiency was obtained in the total absence of BP; that is, polymer brushes were formed on the organic substrate, simply by immersing the substrate in bulk monomer and irradiating it with UV light.

Li et al.²⁰ proposed that the monomer (styrene) itself acts as the photosensitizer and reaches a triplet state upon photon adsorption. This triplet state is in equilibrium with a biradical species ($\cdot\text{St}\cdot$), which initiates a free radical polymerization in solution. However, $\cdot\text{St}\cdot$ can also abstract a hydrogen radical from the organic substrate and thus create a surface radical site for a free radical surface-initiated polymerization of styrene. This mechanism was defined as the self-initiated photografting and photopolymerization (SIPGP). Brown and Wang²¹ presented similar results for the photografting of various acrylic monomers on high density polyethylene substrates. Along this line, some of us reported recently on the preparation of very stable structured polystyrene (PS) brushes directly on ultrananocrystalline diamond by the SIPGP of styrene.²² Surprisingly, this straightforward approach for the preparation of thick polymer brushes has not attracted much attention.

To our best knowledge, the only example of SIPGP on SAMs was reported by Dyer and co-workers.²³ Approximately 200 nm thick PS brushes as well as 675 nm thick poly(methyl methacrylate) (PMMA) brushes were prepared on thiol SAMs on gold with terminal tertiary amine functions. The SAMs were immersed in a monomer solution in the absence of a specific photoinitiator or sensitizer and irradiated with UV light. The authors proposed that the photoactivated monomer activates the amino group by electron transfer or, as outlined above, by hydrogen abstraction. Because no polymer brush formation was observed under analogue reaction conditions on octadecanethiolate SAMs, the authors concluded that the presence of the tertiary amino groups was essential for the SIPGP. However, as Rånby and co-workers demonstrated, the SIPGP can also be performed on polyethylene substrates that contain only *n*-alkanes.

Thus, the different studies^{13,24,11,25} on the photoinitiated SIP of styrene or acrylic monomers on SAMs bearing specific photolabile initiator groups for the free radical polymerization may indicate that surface grafted polymer chains are also formed by a simultaneous SIPGP process. A first hint might be the kinetic studies on surface-initiated photopolymerization (SIPP) by Dyer²⁵ who reported that the increase of the polymer brush thickness with the (irradiation) polymerization time was nonlinear for the SIPP of styrene on AIBN-type functionalized SAMs, leading to the proposal of a complex four-stage growth model. In contrast, Rühle et al.²⁶ as well as our group¹³ reported on the SIPP of styrene from structured aromatic SAMs equipped with asymmetric azo-initiators. In both cases, the polymer brush layer increase was found to be a strictly linear function of the irradiation time. Differences between these studies are—beside the different SAMs used as photoinitiators—the conditions of irradiation, that is, time, spectral distribution, and light intensity. However, it cannot

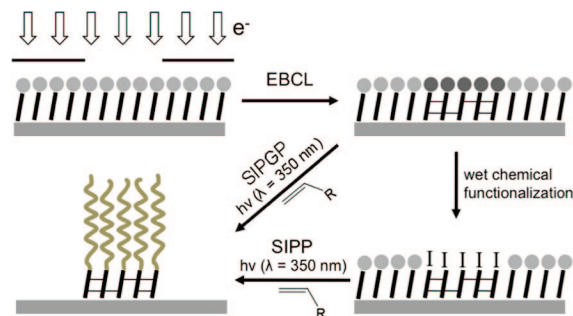


Figure 1. Preparation of structured polymer brushes by SIPGP or SIPP.¹³

be excluded in any of these studies that SIPGP of styrene was at least partially involved in the formation of the polymer structures.

In this work, we investigated SIPGP of styrene and acrylic monomers on various structured ω -functionalized biphenylthiol SAMs on gold which were selectively cross-linked by electron beam chemical lithography (EBCL). We show that the SAM functionalization step for the preparation of a surface bonded initiator is not necessary. Furthermore, the comparison of polymer brushes prepared by SIPP and SIPGP using analogue systems and identical UV irradiation conditions was studied in order to gain insight into the processes involved during the SIPP of vinyl monomers.

The differences between SIPP and SIPGP for the grafting of styrene on a SAM of 4'-nitro-1,1'-biphenyl-4-thiol (NBT) are outlined schematically in Figure 1. While for SIPP the native NBT SAM is converted first to cross-linked cABT and requires the selective conversion to an azo-functionalized (cAMBT) monolayer, SIPGP is performed directly on the electron-irradiated cABT surface.

Experimental Section

SAM Preparation. The synthesis of 4-mercapto-1,1'-biphenyl (BPT), 4'-methyl-1,1'-biphenyl-4-thiol (MBT), 4'-hydroxy-1,1'-biphenyl-4-thiol (HBT), and 4'-nitro-1,1'-biphenyl-4-thiol (NBT), the preparation of the SAMs, the synthesis of methylmalonodinitrile and the surface bonded initiator (4'-azomethylmalonodinitrile-1,1'-biphenyl-4-thiol, cAMBT) were performed as previously reported.^{27,28}

Electron Beam Chemical Lithography (EBCL). A flood gun (100 eV, 60 mC/cm²) was used to irradiate the NBT SAMs through a stencil mask (Quantifoil Micro Tools, Jena, hole radius = 1 μm , center-to-center distance = 4 μm). Direct writing with a focused electron beam was performed with a LEO 1530 scanning electron microscope with Raith Elphy Plus Pattern Generator System (REPGS) software. The electron beam energy was set at 3 keV, vacuum pressure $\sim 5 \times 10^{-6}$ mbar. For the polymer brush gradient experiments, every gradient consisted of 100 parallel $10 \times 0.5 \mu\text{m}^2$ lines with linearly increasing electron dosage. Similarly, the arrays of isolated structures were produced.

Self-Initiated Photografting and Photopolymerization. A freshly prepared SAM (cBPT, cMBT, cHBT, cABT, or cAMBT) was added to approximately 2 mL of freshly distilled and degassed styrene, methyl methacrylate (MMA), or *tert*-butyl methacrylate (tBMA) (Fluka) in a glass photoreaction vial. Polymerization was allowed to complete within different time periods (0–20 h) under irradiation with UV light ($\lambda_{\text{max}} = 350 \text{ nm}$, 9.2 mW/cm^2) in a Rayonet photochemical reaction chamber (Branford, Connecticut) at room

(20) Li, S. J.; Li, C. G.; Li, T.; Cheng, J. J.; *Polymer Photochemistry Principles and Applications*, 1st ed.; Fudan University Press: Shanghai, 1993; p 110.

(21) Wang, H.; Brown, H. R. *Macromol. Rapid Commun.* **2004**, *25*, 1095.

(22) Steenackers, M.; Lud, S. Q.; Niedermeier, M.; Bruno, P.; Gruen, D. M.; Feulner, P.; Stutzmann, M.; Garrido, J. A.; Jordan, R. *J. Am. Chem. Soc.* **2007**, *129*, 15655.

(23) Dyer, D. J.; Feng, J.; Schmidt, R.; Wong, V. N.; Zhao, T.; Yagci, Y. *Macromolecules* **2004**, *37*, 7072.

(24) (a) Paul, R.; Schmidt, R.; Feng, J.; Dyer, D. J. *J. Polym. Sci., Part A: Polym. Chem.* **2002**, *40*, 3284. (b) Schmidt, R.; Zhao, T.; Green, J.-B.; Dyer, D. J. *Langmuir* **2002**, *18*, 1281. (c) Feng, J.; Dyer, D. J. *Polymer Prepr.* **2005**, *46*, 102. (d) Feng, J.; Haasch, R. T.; Dyer, D. J. *Macromolecules* **2004**, *37*, 9525. (e) Niwa, M.; Date, M.; Higashi, N. *Macromolecules* **1996**, *29*, 3681.

(25) Dyer, D. J. *Adv. Polym. Sci.* **2006**, *197*, 47.

(26) Chen, X.; Tolbert, L. M.; Henderson, C. L.; Hess, D. W.; Rühle, J. *J. Vac. Sci. Technol., B* **2001**, *19*, 2013.

(27) Kang, J. F.; Ulman, A.; Liao, S.; Jordan, R.; Yang, G.; Liu, G.-Y. *Langmuir* **2001**, *17*, 95.

(28) Gölzhäuser, A.; Eck, W.; Geyer, W.; Stadler, V.; Weimann, T.; Hinze, P.; Grunze, M. *Adv. Mater.* **2001**, *13*, 806.

temperature. After the polymerization, the samples were removed from the reaction solution and immediately washed with a good solvent for the respective polymer (PS in toluene; PMMA and poly(*t*BMA) in acetone). To ensure that only chemically grafted polymers remained on the surface, all substrates were additionally cleaned by ultrasonication for 5 min in the fresh solvents. The samples were additionally treated by ultrasonication in ethyl acetate and ethanol for 5 min each. This washing procedure was sometimes repeated to remove all contaminations.

Atomic Force Microscopy (AFM). AFM scans were performed with a Nanoscope IIIa scanning probe microscope from Veeco Instruments using standard tips in tapping mode under ambient conditions. The polymer layer thickness of micrometer sized structures prepared with a stencil mask was evaluated from 20 μm^2 scans. The average polymer layer thickness and the given error were obtained by data analysis as previously reported.¹³ The height analysis of the brush gradients and nanometer patterns in the arrays were determined by several detailed scans of smaller sections.

Results and Discussion

Following the study of Dyer²⁵ on the photopolymerization of styrene on amino-functionalized alkylthiol SAMs on gold, we performed an analogue photopolymerization of styrene on biphenyl SAM systems as sketched in Figure 1. In a first set of experiments, a SAM of 4'-nitro-1,1'-biphenyl-4-thiol (NBT) was irradiated with an electron flood gun (50 eV, 60 mC/cm²) through a stencil mask with hole diameter of 2 μm to cross-link 4'-amino-1,1'-biphenyl-4-thiol (cABT) in the irradiated areas. These surfaces were submerged in styrene and irradiated with UV light for different times. The substrates were then intensively washed by ultrasonication in various solvents to ensure that only chemically grafted PS remained on the surface, dried in a jet of nitrogen, and investigated by AFM under ambient conditions. Polystyrene brushes were selectively formed on the irradiated cABT areas.²⁹ The thicknesses of the polymer coatings were uniform, and the layer thickness was found to increase linearly with the photopolymerization time.

The selective grafting of styrene onto cABT monolayers can have two possible reasons: Either SIPGP involving surface radical formation by radical abstraction by a photoactivated monomer only occurs on cABT areas or the conditions of the photopolymerization cause desorption of the non-cross-linked SAM. It is known that thiol SAMs on gold can photooxidize by exposure to UV light.³⁰ However, the SAM photostability depends on several parameters such as wavelength, SAM packing, morphology, and functionality.³¹

To test the stability difference of native to cross-linked biphenyl SAMs, a monolayer of biphenyl thiol (BT) on gold was prepared, irradiated with electrons as described above, submerged in toluene, irradiated with the same UV light source for only 30 min, and then inspected with AFM (Figure 2).

AFM measurements showed that only the isolated cross-linked areas with a layer thickness of $10 \pm 2 \text{ \AA}$ remained on the surface (Figure 3). This value is in good agreement with the theoretical height of a cBT SAM. We thus conclude that non-cross-linked BT molecules desorbed from the surface during the irradiation with intensive UV light (9.2 mW/cm²) while the cBT monolayer

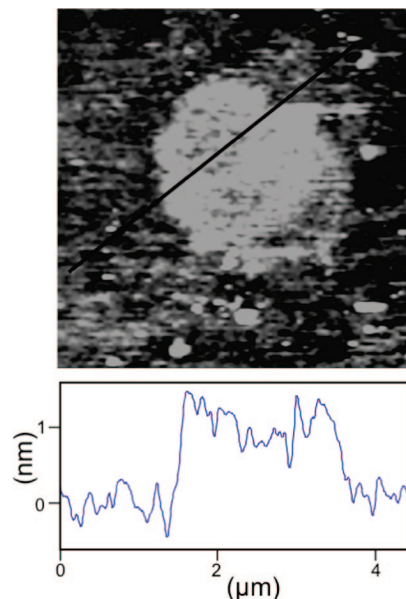


Figure 2. AFM measurement of a structured cross-linked BT SAM (EBCL: 1 μm radius; 50 eV; 60 mC/cm²). The sample was submerged in toluene and irradiated with UV light over a period of 30 min.

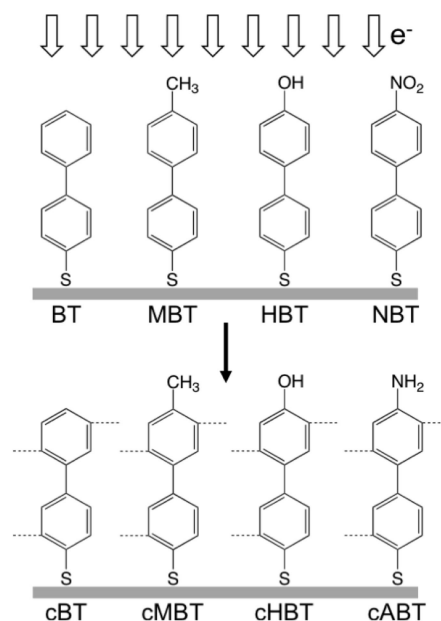


Figure 3. Electron beam irradiation of 4-mercapto-1,1'-biphenyl (BT), 4'-methyl-1,1'-biphenyl-4-thiol (MBT), 4'-hydroxy-1,1'-biphenyl-4-thiol (HBT), and 4'-nitro-1,1'-biphenyl-4-thiol (NBT) SAMs results in cross-linked cBT, cMBT, cHBT, and cABT (4'-amino-1,1'-biphenyl-4-thiol) SAMs.

remained on the surface because of the multiple adhesion sites of the entire cross-linked layer to the substrate.^{32–34}

SIPGP on Different ω -Functionalized Biphenylthiol SAMs. Since the work of Rånby and co-workers,^{17–19} Li et al.,²⁰ Brown and Wang,²¹ and our own work²² suggest that SIPGP of vinyl monomers can be applied on surfaces with various chemical functionalities, we tested different ω -functionalized biphenylthiol SAMs featuring hydrogen, methyl-, hydroxyl-, and amino-functions in the 4'-position (Figure 3).

(29) As a control experiment, we irradiated clean gold substrates with an electron flood gun through a stencil mask. The substrates were immersed in monomer and irradiated with UV light for several hours. In this experiment, no grafted polymer could be observed.

(30) Brewer, N. J.; Janusz, S.; Critchley, K.; Evans, S. D.; Leggett, G. J. *J. Phys. Chem. B* **2005**, *109*, 11247.

(31) Brewer, N. J.; Rawsterne, R. E.; Kothari, S.; Leggett, G. J. *J. Am. Chem. Soc.* **2001**, *123*, 4089.

(32) Geyer, W.; Stadler, V.; Eck, W.; Zharnikov, M.; Götzhäuser, A.; Grunze, M. *Appl. Phys. Lett.* **1999**, *75*, 2401.

(33) Eck, W.; Götzhäuser, A.; Zharnikov, M.; Stadler, V.; Geyer, W.; Grunze, M. *PCT/DE00/03264*, 1999.

(34) Eck, W.; Küller, A.; Grunze, M.; Völkel, B.; Götzhäuser, A. *Adv. Mater.* **2005**, *17*, 2583.

Table 1. PMMA Brush Layer Thickness on Different Cross-Linked SAMs along with the Bond Dissociation Energies (BDEs) Related to the Major 4'-Function^a

SAM	4'-substitution	h_d (nm)	BDE (kcal/mol)
cBT	-H	65 ± 8	111 ^b
cMBT	-CH ₃	82 ± 11	86 ^c
cHBT	-OH/-H	70 ± 10	87.3 ^d
cABT	-NH ₂ /-H	85 ± 11	89.3 ^e

^a Since no experimental or theoretical BDEs for the 4'-functions of cross-linked biphenylthiols are available, we listed here the (higher) BDEs.³⁶ ^b BDE of benzene. ^c BDE of toluene. ^d BDE of aniline. ^e BDE of phenol.

As described above, the native BT, MBT, and HBT SAMs were structured/cross-linked by electron irradiation through a stencil mask with an electron flood gun (electron energy = 50 eV, electron dosage = 60 mC/cm²). It is known from the literature that electron beam irradiation of ω -functionalized biphenylthiol SAMs causes lateral cross-linking of the biphenyl mesogen: BT, MBT, and HBT are converted into cross-linked cBT,³³ cMBT,³⁵ and cHBT,²⁸ respectively. In addition to cross-linking, the nitro-function of NBT is converted to an amino-functionalized cABT SAM (Figure 3).³³

The different substrates were submerged in one reaction vessel with methyl methacrylate as the monomer and irradiated for 16 h with UV light. In all cases, PMMA polymer brushes were selectively formed on the cross-linked SAM regions, while non-cross-linked SAMs desorbed during UV irradiation. Table 1 summarizes the resulting layer thicknesses of PMMA brushes created by the SIPGP of MMA on the cross-linked SAMs having different 4'-functionalities.

Since SIPGP relies on the creation of surface radical sites via radical abstraction by a photoactivated monomer, the grafting efficiency and thus the resulting polymer brush thickness should be correlated to the bond dissociation energies of the different surface functions. In previous studies, this explained the selective grafting of styrene on oxidized and H-terminated diamond substrates using the SIPGP process.²² However, as is apparent from Table 1, no direct correlation can be established. One reason may be that the electron beam irradiation not only cross-links the biphenyl monolayers and reduces NBT to a cABT monolayer but also simultaneously desorbs fractions of the 4'-substituent and, at increasing electron dose, converts the aromatic phenyl rings to a (cross-linked) hydrocarbon framework. For example, the methyl group of MBT SAMs is believed to remain unaffected during the electron beam induced cross-linking reaction while the extensive irradiation of HBT SAMs causes partial OH abstraction.^{35,28} In other words, the surface concentration of the 4'-function is most likely not identical for the different cross-linked ω -functionalized biphenylthiol SAMs.

The experiments clearly show that SIPGP can be performed for the preparation of well-defined polymer brushes, not only of styrene but, for example, also of MMA on substrates having diverse functional groups such as amines, *n*-alkanes, phenyls, and hydroxyls. However, required is the presence of surface functionalities from which (hydrogen) radicals can be abstracted by a photoactivated monomer, that the successively formed surface-bonded radicals can initiate a free radical polymerization, and that the surface coupling of the entire layer is stable under UV irradiation.

(35) Kornjakov, A.; Küller, A.; Gupta, P.; Loos, K.; Spagnoli, C.; Ulman, A.; Eck, W.; Grunze, M. Unpublished results.

(36) BDEs of benzene and toluene: Yang, W. T.; Rånby, B. *Polym. Bull.* **1996**, *37*, 89. Aniline: Jonsson, M.; Lind, J.; Eriksen, T. E.; Merényi, G. *J. Am. Chem. Soc.* **1994**, *116*, 1423. Phenol: Wright, J. S.; Carpenter, D. J.; McKay, D. J.; Ingold, K. U. *J. Am. Chem. Soc.* **1997**, *119*, 4245.

Polymer Brush Gradients by SIPGP on Cross-Linked Biphenyl Thiol (cBT). As outlined above, non-cross-linked BT SAMs selectively desorb from the gold substrate under UV irradiation and SIPGP produces PMMA brushes from cBT SAMs. Since the extent of the electron-induced cross-linking reaction is dependent on the locally applied electron dose, surface gradients of BT/cBT can be produced by direct writing using a focused electron beam, thus resulting in SAM areas of increasing UV stability. A successive SIPGP reaction then occurs on a surface with increasing grafting sites and thus results in polymer brushes gradients. This is the analogue SIPGP process to the recently reported SIPP approach for the fabrication of polymer brush gradients using EBCL and concentration gradients of surface bonded azo-functions.¹³

On a single substrate, a BT SAM was irradiated with a focused electron beam with a linearly increasing dose from 0 to 11, 0 to 37.5, and 0 to 110 mC/cm² to create biphenyl SAMs of increased cross-linking over three areas of 10 × 50 μ m² each. The gradient substrate was irradiated for 16 h with UV light in bulk styrene. The AFM scan of the carefully cleaned substrate is shown in Figure 4, along with the height profile of the resulting structures.

As expected, SIPGP occurred on the locally cross-linked cBT SAM areas and nonirradiated BT desorbed under UV irradiation, leaving a bare gold surface behind. It is apparent that the resulting dry PS brush thickness is determined by the locally applied electron dose and thus to the extent of monolayer cross-linking. From comparison of the three gradients, it follows that the polymer layer thickness at a given electron beam dosage is almost identical for the three gradients, for example, the average polymer layer thickness at 8 mC/cm² is 38.5 nm in the first gradient, 37.5 nm in the second gradient, and 38.4 nm in the third gradient structure.

In general, the thickness of dry (collapsed) polymer brushes is given by

$$h_d = M_n \sigma / \rho N_A \quad (1)$$

where M_n , σ , and ρ are, respectively, the molecular weight, grafting density, and bulk density of the grafted polymer and N_A is the Avogadro constant.¹³ Since the reaction conditions were identical for all structures, the increase of the polymer layer thickness has to be attributed to the increase of the polymer grafting density.

The absence of polymer brushes at electron beam doses lower than 2 mC/cm², as observed in the upper gradient in Figure 4, is attributed to the insufficient cross-linking of biphenyl mesogen at very low electron beam dosage resulting in UV-induced desorption of the SAM. Between 2 and 5 mC/cm², PS brushes cover the surface only partially and only some cross-linked *islands* remained attached to the gold surface. This can be observed very clearly in the first 0 to 11 mC/cm² gradient (Figure 4). Furthermore, the growth of polymer chains from partially cross-linked SAMs with few anchor points will result in desorption of entire patches due to the additional entropic pressure by the surface grafted chains. At higher electron doses, a thicker and homogeneous PS brush is formed. The polymer layer thickness increases to a value of approximately 105 nm for areas exposed to approximately 50 mC/cm². The maximum polymer layer thickness is attributed to a fully cross-linked cBT monolayer and thus the maximum grafting density of the polymer brushes. Above 50 mC/cm², the polymer layer thickness remains constant.

As in our previous work on gradients produced by SIPP, the experimental dry polymer layer thickness can be fitted exponentially as a function of the irradiation dosage D :

$$h_d(D) = h_{d0} [1 - \exp(-D'/D_0)] \quad (2)$$

where h_{d0} is the maximum polymer layer thickness. D_0 describes the efficiency of the process. D' is the onset corrected dosage.

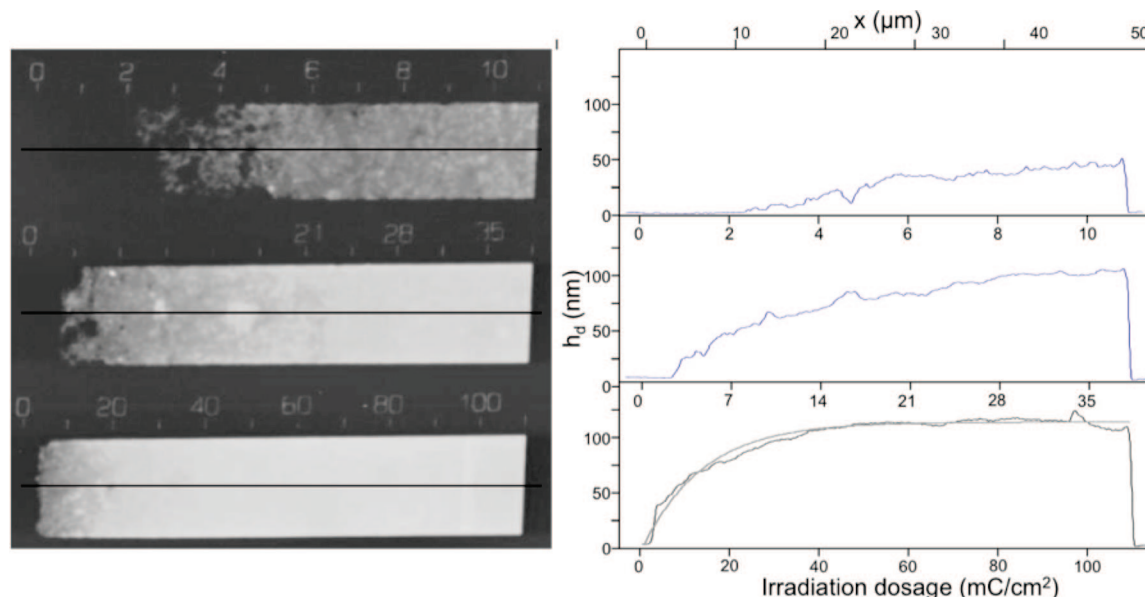


Figure 4. AFM image ($52 \times 52 \mu\text{m}^2$) and height profile of three PS gradients on a cBT monolayer on a single same substrate. The electron beam dosage increases linearly from 0 to 11, 0 to 37.5, and 0 to 110 mC/cm^2 ($t_p = 16$ h). In the height profile of the 0 to 110 mC/cm^2 gradient, an exponential fit function is plotted as a black solid line (see text for details).

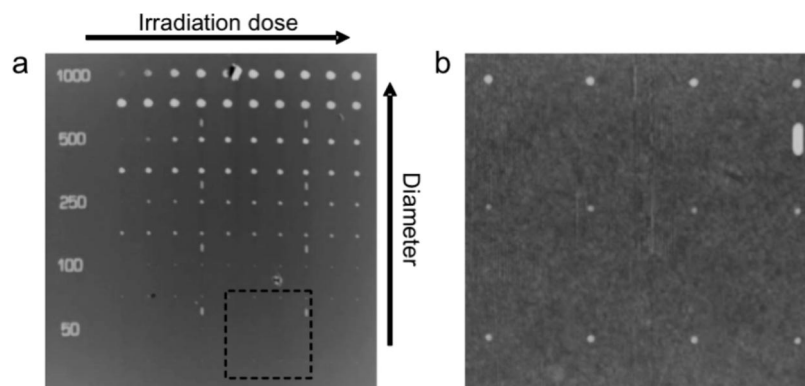


Figure 5. (a) AFM scan ($55 \times 55 \mu\text{m}^2$) of the PS structure matrix formed by SIPGP directly on cABT SAMs, with variation of the structure size from 1 μm to 50 nm and different irradiation doses from 5 to 100 mC/cm^2 . (b) Detailed AFM scan ($14.43 \times 14.43 \mu\text{m}^2$) of 50 nm PS structures as indicated in (a).

The onset is caused by the absence of polymer brushes at very low electron beam doses as discussed above. The values for the fit function in Figure 5 are $h_{d0} = 112$ nm, $D' = D - 1.5$ mC/cm^2 , and $D_0 = 13.5$ mC/cm^2 .

Comparing these gradients prepared by SIPGP with our previous results on the morphology control of PS brushes created by the SIPP technique,¹³ the resulting dry layer thickness of the gradient as a function of the electron beam irradiation dose is significantly different. This may be due to the different electroninduced cross-linking of the two SAMs, their 4'-functionality, and/or the initial polymer grafting mechanism. To elucidate this aspect and to determine the effect of the presence of a 4'-azo function, SIPG was performed on cross-linked cABT SAMs.

SIPP versus SIPGP. Analogous to our previous report,¹³ NBT SAMs on gold were structured by EBCL to form a defined pattern NBT/cABT array with diameters from 50 nm to 1 μm and electron dosages between 5 and 100 mC/cm^2 . The structured ABT/cABT SAMs were submerged in bulk styrene and irradiated with the same UV source as that used for all other experiments (including the work in ref 13) for 16 h.

The AFM investigation of the array (Figure 5) shows that the amplification of the structured cABT by SIPGP to thick polymer

brush structures is selective on all length scales and even amplifies small cross-linked cABT areas of 50 nm.

Analysis of the brush height as a function of the used electron dose (Figure 6) gives an analog trend as described previously for the PS array prepared by SIPP using an azo-functionalized SAM.¹³ For both SIPP and SIPGP, the polymer layer height increases with higher electron dosage (increased SAM cross-linking and amino group concentration) to a maximum around 35 mC/cm^2 and then steadily decreases due to the loss of the 4'-amino functionality (cABT to cBT conversion). For nanoscaled structures, no significant differences between the SIPP with and SIPG without a surface initiator is observable; however, for larger structures (e.g., 0.5 and 1 μm dot diameter), the polymer layers prepared directly on cABT are significantly thicker, especially for structures with maximum lateral amino group concentrations.

In fact, the direct comparison of the results in this study with our former experimental data¹³ suggest that the SIPGP mechanism is so effective and selective that an additional introduction of surface azo groups is not needed to prepare defined polymer brush structures on various monolayers or coatings. Moreover, the additional wet chemical process may contaminate or alter the surface as such that potential grafting sites for the simultaneously occurring SIPGP mechanism are reduced. This might explain

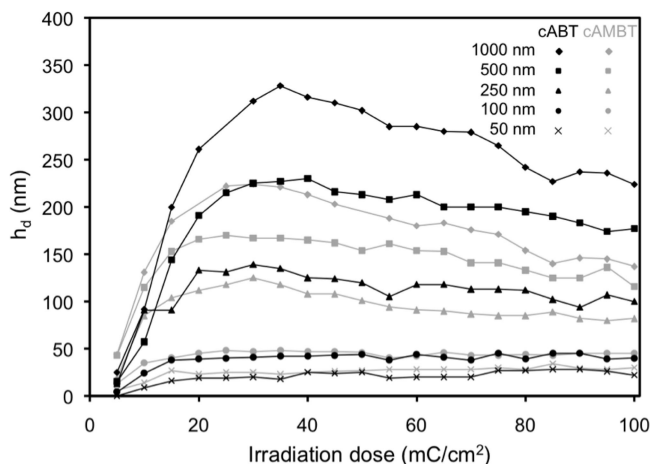


Figure 6. PS brush height as a function of structure size and electron irradiation dose from the array in Figure 5 prepared by SIPGP of styrene from cABT (solid points and lines) along with data from our previous study (see ref 13) for direct comparison.

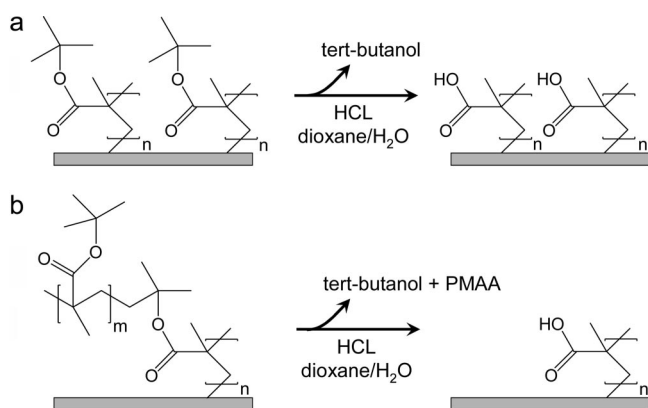


Figure 7. Hydrolysis of PtBMA brushes results in PMAA brushes and *tert*-butanol. The hydrolysis of branched PtBMA brushes (b) results in the cleavage of more grafted material compared to the hydrolysis of linear PtBMA brushes (a).

the significantly lower brush thickness at areas of high amino functionalities in the SIPP gradient for the region around 35 mC/cm².

In conclusion, the comparison of the polymer brushes created by the SIPP of styrene on cAMBT SAMs¹³ and the SIPGP of styrene and MMA on cBT, cMBT, cHBT, and cABT SAMs under identical UV irradiation conditions shows that highly defined polymer brush structures such as gradients and micro- and nanostructures with predetermined thicknesses can be created without specific surface-bonded initiators.

Molecular Architecture of Polymer Brushes Prepared by SIPGP. Since hydrogen radicals can be abstracted from diverse surface functionalities, it is very likely that during the photopolymerization hydrogen radicals are also abstracted by photoactivated monomer biradicals from already grafted polymer chains, resulting in the formation of branched polymer grafts.

To check for the presence of branched polymer chains, the polymer architecture was studied indirectly by investigating the influence of hydrolyzation of the ester group in structured poly(*tert*-butyl methacrylate) (PtBMA) brushes on the dry polymer layer thickness. The hydrolyzation of PtBMA brushes results in poly(methacrylic acid) (PMAA) brushes as schematically shown in Figure 7.

In case the SIPGP results in mostly linear PtBMA brushes, hydrolysis to PMMA would only slightly change the grafting

density σ and the average molar mass (M_n) of the grafted chains would decrease by 39.5%, due to the cleavage of the pendant *tert*-butyl group (Figure 7a). Furthermore, the bulk density, ρ , decreases by 7.5% when amorphous PtBMA is hydrolyzed to PMAA.³⁷ When the dry thickness of linear PtBMA brushes (h_{d1}) is known, the expected PMAA thickness (h_{d2}) after hydrolyzation can be calculated using eq 1:

$$h_{d2} = \frac{h_{d1}\rho_1M_{n2}}{M_{n1}\rho_2} \quad (3)$$

According to eq 3, a quantitative hydrolyzation of linear PtBMA brushes would result in a thickness decrease of approximately 33%.

However, a greater thickness decrease would be expected for the hydrolyzation of branched PtBMA chains. If the branching occurs partly on the *tert*-butyl group, the hydrolysis of the ester function would result in the desorption of entire polymer chains (Figure 7b) and the thickness decrease of the polymer brush would be significantly higher.

The following experiment was performed: 155 ± 10 nm thick patterned PtBMA brushes were created by immersing structured cABT SAMs in *t*BMA and irradiated with UV light for 5 h. The ester group was then hydrolyzed by placing the sample in refluxing HCl/dioxane/water (2:3:4 volume ratio) for 3 h. After hydrolyzation, the sample was intensively rinsed and dried, and the polymer layer thickness was measured.

According to eq 3, the hydrolyzation of 155 nm thick linear PtBMA brushes would result in approximately 103 nm thick PMAA brushes; however, in our experiment, a thickness of the hydrolyzed PtBMA brush of 75 ± 10 nm was measured which corresponds to a thickness decrease of approximately 52%. The significant thickness decrease, due to hydrolyzation of the ester group, is a strong indication that PtBMA brushes formed by SIPGP have a branched architecture.³⁸

In the light of these experiments as well as the investigations made on the various functionalized SAMs and SAM gradients, we can also conclude that the polymer brushes prepared by the surface-initiated photopolymerization (SIPP) using surface-bonded photoinitiator functions as reported by various research groups have a branched architecture because the SIPGP mechanism occurs not only on the primary organic coating (SAM) but also on the growing/grafted polymer chains. Since SIPP is normally performed over UV irradiation times of several hours, the degree of branching can be significant.

Conclusions

It has been demonstrated that self-initiated photografting and photopolymerization (SIPGP) of styrene and acrylic monomers on structured ω -functionalized biphenylthiols SAMs on gold is a straightforward three-step approach which allows the preparation of defined structured polymer brushes without the need of a specific surface bonded photoinitiator function. Polymer brushes were selectively formed on cross-linked SAM regions, while non-cross-linked SAM molecules desorbed from the gold substrate by UV irradiation. Furthermore, the polymer layer thickness can be directly controlled by the extent of electron-induced cross-linking and head group conversion of the SAM layer. SIPGP was successful on benzyl-, phenyl-,

(37) Bandrup, J.; Immergut, E. H. *Polymer Handbook*, 3rd ed.; Wiley: New York, 1989.

(38) To control the stability of the polymer brushes under these hydrolyzation conditions, a sample with PS brushes on structured cABT SAMs was treated under identical reaction conditions. No significant thickness decrease of the PS brushes could be observed.

hydroxyl-, and amino-functionalized cross-linked SAMs. In general, this indicates that, during SIPP of styrene and acrylic monomers on surface-bonded initiators, the surface-attached radicals are formed not only by photoactivation of the initiator groups but also by the abstraction of hydrogen atoms from surface functionalities through photoactivated monomers. Furthermore, it was shown that that polymer brushes obtained by the SIPGP process have a branched architecture.

Acknowledgment. The authors acknowledge the financial support by the Deutsche Forschungsgemeinschaft via Projects

JO287/2-1 and GR625/50-1 as well as via the SFB 563 "Bioorganic Functional Systems on Solids". M.G. additionally is thankful for financial support by the EU Integrated Project "Ambio." M.S. is grateful for a PostDoc stipend from the Wacker-Institut für Siliciumchemie of the TU München, and R.J. for the financial support of the corresponding project.

LA803386C